Multi-modal causality analysis of eyes-open and eyes-closed data from simultaneously recorded EEG and MEG

Abdul Rauf Anwar[1*], Kidist Gebremariam Mideska[1], Helge Hellriegel[2], Nienke Hoogenboom[3],
Holger Krause[3], Alfons Schnitzler[3], Günther Deuschl[2], Jan Raethjen[2], Ulrich Heute[1],
and Muthuraman Muthuraman[2]

Abstract— Owing to the recent advances in multi-modal data analysis, the aim of the present study was to analyze the functional network of the brain which remained the same during the eyes-open (EO) and eyes-closed (EC) resting task. The simultaneously recorded electroencephalogram (EEG) and magnetoencephalogram (MEG) were used for this study, recorded from five distinct cortical regions of the brain. We focused on the 'alpha' functional network, corresponding to the individual peak frequency in the alpha band. The total data set of 120 seconds was divided into three segments of 18 seconds each, taken from start, middle, and end of the recording. This segmentation allowed us to analyze the evolution of the underlying functional network. The method of time-resolved partial directed coherence (tPDC) was used to assess the causality. This method allowed us to focus on the individual peak frequency in the 'alpha' band (7-13 Hz). Because of the significantly higher power in the recorded EEG in comparison to MEG, at the individual peak frequency of the alpha band, results rely only on EEG. The MEG was used only for comparison. Our results show that different regions of the brain start to 'disconnect' from one another over the course of time. The driving signals, along with the feedback signals between different cortical regions start to recede over time. This shows that, with the course of rest, brain regions reduce communication with each another.

I. INTRODUCTION

Since the discovery of the alpha rhythms in EEG, by Hans Berger in 1929, research on brain signals have paced significantly [1]. These advances have led to the innovation of various modalities to measure the brain activity. Such modalities include magnetoencaphelography (MEG) in 1968 [2], magnetic resonance imaging (MRI) in 1973 [3], near-infra-red spectroscopy (NIRS) in 1977 [5], and functional magnetic-resonance imaging (fMRI) in 1990 [4]. All of these aforementioned modalities use different principles of the brain anatomy to explore and analyze the brain activity. Due to this fact, different modalities can be used simultaneously to complement one another. For example, EEG and fMRI can be used simultaneously to better capture both the time and spatial dynamics of brain activity, since EEG has better temporal resolution and fMRI offers good spatial resolution. Such multi-modal analyses have also been auspicious in recent past because they can help us to better understand the effective properties, anatomy, physiology and dynamics of the brain [6], [7], [8], [9]. Principally, both EEG and MEG fields have the same signal source, i.e., currents in the brain, since every electrical field produces an orthogonal magnetic field. It is clear that every EEG field will have corresponding MEG field. However, because of the fact that the resulting MEG is orthogonal to the EEG, both EEG and MEG capture different components of the brain activity. EEG is reported to be good at capturing radial current sources in the brain, whereas MEG is said to be better at capturing tangential component of fields produced by the brain signals [10]. Hence, using both EEG and MEG simultaneously seems to be the optimal choice for comprehensively capturing brain activity. One important aspect of the brain-signal analysis is to understand what is happening at the functional level in the brain. Different classical models, such as structural equation modeling (SEM) and multivariate auto-regressive modeling (MVAR), exist to analyze such effective connectivity in the brain [11]. MVAR-model-based connectivity analyses include time-domain methods, e.g., Granger-causality index, and frequency-domain methods like directed transfer function (DTF) and partial directed coherence (PDC) [12].

II. METHODS

The aforementioned methods assume the subjected time series to be stationary; however, in reality, the bio-medical time series need not necessarily be stationary. In order to clarify this, let us consider a general expression for an auto-regressive (AR) model with order p,

$$x_i(t) = \sum_{r=1}^{r=p} a_{ij,r} x_j(t-r) + \eta(t). \qquad (1)$$

Equation (1) describes a stationary process, in which the influence of time series x_j on x_i is weighted by model coefficients $a_{ij,r}$. The model order p shows the memory of the system or in simple words, how many past values

of x_j will influence the present value of x_i. Moreover, model coefficients are independent of time. Once these model coefficients are estimated, they are Fourier transformed and normalized to give the following expression of partial directed coherence [13],

$$|\pi_{i \leftarrow j}(\omega)| = \frac{|A_{ij}(\omega)|}{\sqrt{\sum_k |A_{kj}(\omega)|^2}}. \qquad (2)$$

Here $|\pi_{i \leftarrow j}(\omega)|$ is the magnitude of the partial directed coherence, showing the strength of information flow from time series x_j to x_i at frequency ω. A_{ij} is the Fourier transform of the model coefficients $a_{ij,r}$. Because of the normalizing term in the denominator of Equation (2), the value of PDC is bounded between zero and one. A zero value showing no information flow, while one depicts the maximum flow of information between the time series. In case of non-stationary time series, Equation (1) will become

$$x_i(t) = \sum_{r=1}^{r=p} a_{ij,r}(t)x_j(t-r) + \eta(t). \qquad (3)$$

Estimation of these time-varying model coefficients is challenging, and one method of calculating them is the state-space modeling. A state-space model for a non-linear system can be given as [14],

$$x(t+1) = F[x(t), w] + Bv(t), \qquad (4)$$

$$y(t) = Cx(t) + n(t). \qquad (5)$$

Here, $v(t)$ and $n(t)$ are process and observation noises, respectively. Both noises can be assumed to be Gaussian and white. F is the function of model weights and system states, while C is the observation matrix. Our goal is the measure the parameters of the non-linear model, w. In order to do so, we first have to estimate the hidden states $x(t)$ of the system by using only the information of the observed time series $y(t)$. Hence the problem at hand is to estimate both the model and the state. We do so by employing a *dual extended Kalman filter* (DEKF), in which two Kalman filters are running in parallel with each other. One Kalman filter estimates the state of the system using the information of the current model estimate, while the second Kalman filter estimates the model of the system by using the information of the current states of the system. Details about DEKF can be found elsewhere [15].

Prior to estimating these coefficients, their optimum number has to be determined. This optimum number is known as model order; it should be a compromise between high model accuracy and low complexity. There are numerous methods to determine the model order, such as Akaike's information criterion (AIC) [16] or the Bayesian information criterion (BIC) [17]. AIC is based on the idea of choosing the model that gives the minimum Kullback-Leibler information entropy between fitted model and true data [16]. We estimated the optimum model order using AIC in our study. Then we calculated time-varying model coefficients using DEKF, and we calculated the PDC at each time point and finally concatenated all PDC vectors to make a time-frequency plot of time-resolved partial directed coherence (tPDC) [14]. Time resolved partial directed coherence is able to reveal the time dynamics of all connections against all resolve-able frequencies. Hence using tPDC we can focus on specific connection time dynamics for the frequency of our choice.

III. DATA ACQUISITION

EEG and MEG were recorded simultaneously from 12 healthy subjects during eyes-open (EO) and eyes-closed (EC) paradigm. EEG was recorded using a 128-electrode EEG cap at a sampling rate of 1000 Hz for 120 seconds. For EEG signals, a band-pass filter between 0.01-200 Hz was used to remove very high frequency artifacts and very low frequency trends. The MEG, along with EEG, was recorded using a Neuromag-Elekta system with 306 gradiometers and magnetometers. Out of the one magnetometer and two gradiometers located at one position, the magnetic sensor with highest power at the individual peak frequency of the alpha band was chosen. The resulting MEG signal was digitized with a sampling rate of 1000 Hz.

After the pre-processing of EEG and MEG, five electrodes in case of EEG were chosen to represent five cortical areas of the brain, namely, frontal (F), temporal (T), parietal (P), occipital (O) and central (C). We chose these five regions of the brain for the analysis of functional connectivity between them because all of these are cortical areas, which can be easily recorded by EEG/MEG. Five corresponding magnetic sensors were also selected for MEG. The selection criterion for EEG and MEG sensors was their relative high SNR. Afterwards, three epochs of 18 seconds of data were taken from each electrode/coil time series as shown in Fig. 1.
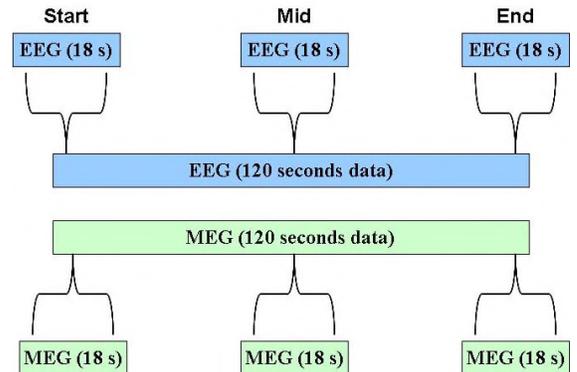

Fig. 1. Segmentation of EEG and MEG data. Eighteen-seconds data epochs were taken from start, middle and end of the recording, both in EEG and MEG.

This process divided the data set into three epochs, namely, start, mid, and end. Individual power spectra of each time series were calculated and the frequency of maximum amplitude within the alpha (7-13 Hz) range was estimated. This frequency is our frequency of choice for the rest of the analysis. We believe that focusing on this frequency will help us to understand the 'alpha' network that remains the same between EO and EC. We applied an appropriate AR model to individual data sets and calculated tPDC for both EO and EC

using EEG and MEG modalities on the time series recorded from five regions of the brain. The optimum model order 'p' was chosen to be fixed for all subjects. As a test for consistency of the applied model, the correlation structures of actual data and simulated data, with similar parameters, were compared. Time-dynamics vectors corresponding to the above described frequency in the alpha range were stored and Spearman's rank correlation was calculated between EO and EC. Our justification for doing so is that we only wanted to analyze the network that remains the same between EO and EC. An example of how tPDC time-frequency plots look like is shown in Fig. 2:
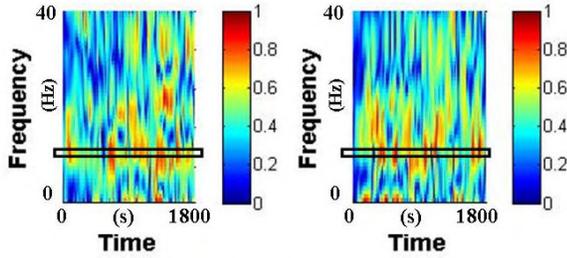

Fig. 2. An example of tPDC time-frequency plot, from MEG and taken from the end epoch of a data set, for both EC (left) and EO (right). Frequency is shown on the y-axis while time is given on the x-axis. Time-dynamics vectors corresponding to strongest alpha-frequency (shown by black rectangle) were correlated to analyze the functional network.

IV. RESULTS

In our study, to quantify differences between EEG and MEG powers, we performed two sample t-tests between them for both EO and EC. The results of the t-tests can be seen in Table I and Table II. The p-value for the t-test was set to 0.005 and all values were found to be significant. This means that the selected EEG electrodes have significantly higher power, at the individual peak frequency in the alpha band, than the MEG sensors. The significance value for the Spearman's rank correlation was set to ($p < 0.01$) for comparing EO and EC vectors. Since we had 12 subjects, we calculated the average of all significant correlations after calculating their Fischer scores. The Kruskal-Wallis test was performed between EEG and MEG tPDC vectors to identify those connections which have significantly ($p < 0.01$) high coherence in case of EEG in contrast to MEG. By doing so, we further validated our results of EEG by comparing them with another modality (MEG). This procedure was repeated for all three data sets, i.e., start, mid, and end. Finally, the functional network during each phase, i.e., start, mid, and end for all five regions of the brain was revealed as shown in Fig. 3. We can see that during the course of recording, all regions of the brain were communicating with each other; however, as time passed, more regions started to alienate from each another. This can be further quantified by calculating the number of uni-directional and bi-directional connections between different regions of the brain over the course of time.

TABLE I

MEAN AND STANDARD DEVIATION FOR 12 SUBJECTS FOR EEG AND MEG PEAK POWER, AT ALPHA FREQUENCY BAND, FOR EYES CLOSED. IN EEG-X-C, X STANDS FOR CORTICAL REGION OF THE BRAIN AND C STANDS FOR EYES CLOSED PARADIGM.

	Mean	N	Std. Deviation	p-value/pair
EEG-F-C	34.9700	12	11.37961	0.004
MEG-F-C	24.7493	12	6.89648	
EEG-T-C	36.3183	12	7.54387	0.000
MEG-T-C	28.4351	12	7.91739	
EEG-P-C	41.8601	12	6.93037	0.000
MEG-P-C	26.8275	12	5.70203	
EEG-O-C	42.4383	12	4.42379	0.000
MEG-O-C	32.4427	12	6.60586	
EEG-C-C	39.9476	12	10.93714	0.004
MEG-C-C	30.8536	12	6.56366	

TABLE II

MEAN AND STANDARD DEVIATION FOR 12 SUBJECTS FOR EEG AND MEG PEAK POWER, AT ALPHA FREQUENCY BAND, FOR EYES OPEN. IN EEG-X-O, X STANDS FOR CORTICAL REGION OF THE BRAIN AND O STANDS FOR EYES CLOSED PARADIGM.

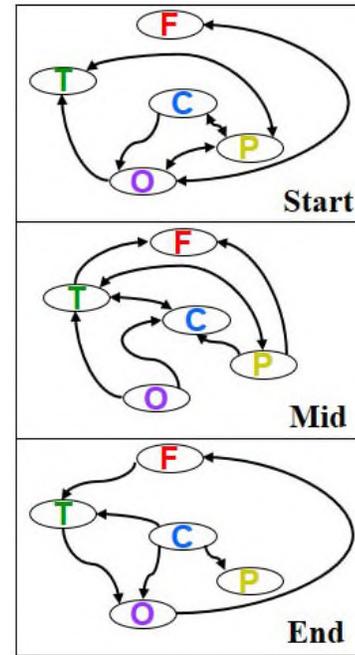|	Mean	N	Std. Deviation	p-value/pair
EEG-F-O	31.7358	12	8.53740	0.001
MEG-F-O	23.2552	12	6.83814	
EEG-T-O	32.9973	12	6.49492	0.000
MEG-T-O	26.0095	12	8.00622	
EEG-P-O	38.8810	12	7.24186	0.000
MEG-P-O	25.1162	12	5.29547	
EEG-O-O	39.8960	12	6.79872	0.000
MEG-O-O	28.3622	12	5.33419	
EEG-C-O	36.8255	12	8.61198	0.000
MEG-C-O	26.6248	12	5.86695	

Fig. 3. EEG connection details: connections between frontal (F), temporal (T), central (C), occipital (O), and parietal (P) regions of the brain. Uni-directional arrows show the connection in one direction. Two-headed arrows show bi-directional connections. The largest number of uni-directional and bi-directional connections appears at the start. During the course of time, the number of connections reduces.

TABLE III

NUMBER OF UNI-DIRECTIONAL AND BI-DIRECTION CONNECTIONS,
DURING START, MID, AND END OF THE RECORDING.

	Uni-directional	Bi-directional
Start	10	4
Mid	9	2
End	6	0

The numbers of bi-directional and uni-directional connections are summarized in Table III. The analysis of the number of connections over the course of recording gives a clear picture of the evolution of the functional network. We see that, in the start, there were total of 10 significant connections between five regions of the brain; out of these 10, 4 were bi-directional. A bi-directional connection shows that both source and destination are communicating with each another in a forward-feedback loop. In the middle part of the recording, the total number of connections reduces to 9, the number of bi-directional connections reduce to two. This shows that the information flow between regions has started to cease along with the forward-feedback loops between them. Finally, in the end phase of the recording, number of connections is significantly reduced in comparison to that of the start phase. Moreover now, there are only uni-directional connections and all bi-directional connections have ceased.

V. CONCLUSIONS

In this study, we analyzed the 'alpha' functional network between five regions of the brain that remains the same during EO and EC, using EEG and MEG. The method used to analyze the causality network was tPDC, which gives both the time and frequency dynamics of causal connections between different regions of the brain. We validated the common network between EO and EC by calculating correlation between their time-dynamics tPDC vectors corresponding to individual alpha-peak frequencies. In addition to this, we also used a comparison of EEG and MEG modalities and showed results for EEG. We observed reduced functional connectivity between five cortical areas under the course of time. Moreover, near the end of recording, the central region of the brain begins to act as a hub for the outgoing connections because it could act as a pacemaker for the eyes open task in the brain. We hypothesize that, as subjects descent to pre-sleep mode, the functional network between these five regions of the brain starts to integrate similarly to the reduced connectivity during sleep [18] [19]. Further studies need to be undertaken for better understanding the functional networks in the brain during resting state.

ACKNOWLEDGMENT

REFERENCES

[1] J. L. Stone, J. R. Hughes, Early history of electroencephalography and establishment of the American clinical neurophysiology society, Journal of Clinical Neurophysiology, vol. 30, no. 1, pp. 28 - 44, 2013.

[2] D. Cohen, Magnetoencephalography: evidence of magnetic fields produced by alpha rhythm currents., Science, vol. 161, pp. 784 - 786, 1968.

[3] A. L. Scherzinger, W. R. Hendee, Basic principles of magnetic resonance imaging, an update, The Western Journal Of Medicine, vol. 143, no. 6, pp. 782 - 792, 1985.

[4] S. Ogawa, T. M. Lee, A. R. Kay, D. W. Tank, Brain magnetic resonance imaging with contrast dependent on blood oxygenation., Proceedings of the National Academy of Sciences of the United States of America, vol. 87, no. 24, pp. 9868 - 9872, 1990.

[5] J. M. Murkin and M. Arango, Near-infrared spectroscopy as an index of brain and tissue oxygenation., British Journal of Anaesthesia, vol. 103, no. 1, pp. 3 - 13, 2009.

[6] J. Suia, T. Adalib, Q. Yua, J. Chena, V. D. Calhouna, A review of multivariate methods for multimodal fusion of brain imaging data., Journal of Neuroscience Methods, vol. 204, no. 1, pp. 68 - 81, 2012.

[7] H. Sato, N. Yahata, T. Funane, R. Takizawa, T. Katura, H. Atsumori, Y. Nishimura, A. Kinoshita, M. Kiguchi, H. Koizumi, M. Fukuda, K. Kasai, A NIRS - fMRI investigation of prefrontal cortex activity during a working memory task, NeuroImage, vol. 83, pp. 158 - 173, 2013.

[8] S. Baumeister, S. Hohmann, I. Wolf, M. Plichta, S. Rechtsteiner, M. Zangl, M. Ruf, N. Holz, R. Boecker, A. Meyer-Lindenberg, M. Holtmann, M. Laucht, T. Banaschewski, D. Brandeis, Sequential inhibitory control processes assessed through simultaneous EEG - fMRI., NeuroImage, 2014.

[9] K. Keuper, P. Zwitserlood, M. A. Rehbein, A. S. Eden, I. Laeger, M Junghfer, P. Zwanzger, C. Dobel, Early Prefrontal Brain Responses to the Hedonic Quality of Emotional Words - A Simultaneous EEG and MEG Study, PLoS One., vol. 8, no. 8, e70788., 2013.

[10] D. Sharon, M. S. Hämäläinen, R. B. H. Tootell, E. Halgren, J. W. Belliveau, The advantage of combining MEG and EEG: Comparison to fMRI in focally stimulated visual cortex, J Sleep Res., vol. 36, no. 4, pp. 1225 - 1235, 2007.

[11] K. E. Stephen, K. J. Friston, Analyzing effective connectivity with fMRI, Wiley Interdiscip. Rev. Cogn. Sci., vol. 1, no. 3, pp. 446-459, 2010.

[12] K. J. Blinowska, Review of the methods of determination of directed connectivity from multichannel data, Med. & Biol. Engin. & Comput., vol. 49, no. 5, pp. 521-529, 2011.

[13] B. Schelter, L. Sommerlade, B. Platt, A. Plano, M. Thiel, J. Timmer, Multivariate analysis of dynamical processes with applications to the neurosciences, Engineering in Medicine and Biology Society, EMBC, 2011 Annual International Conference of the IEEE, vol., no., pp.5931 - 5934, Aug. 30 2011-Sept. 3 2011.

[14] A. R. Anwar, M. Muthalib, S. Perrey, A. Galka, O. Granert, S. Wolff, G. Deuschl, J. Raethjen, U. Heute, M. Muthuraman, Comparison of causality analysis on simultaneously measured fMRI and NIRS signals during motor tasks, Engineering in Medicine and Biology Society (EMBC), 2013 35th Annual International Conference of the IEEE , vol., no., pp.2628-2631, 3-7 July 2013.

[15] E. A. Wan, A. T. Nelson, Kalman Filtering and Neural Networks , John Wiley & Sons, Inc., 2002, ch. 5.

[16] H. Akaike, A new look at the statistical model identification, Automatic Control, IEEE Transactions on , vol. 19, no. 6, pp. 716-723, Dec 1974.

[17] G. Schwarz, Estimating the dimension of a model, The annals of statistics, vol. 6, no. 2, pp. 461-464, 1978.

[18] V. I. Spoormaker, P. Gleiser, M. Czisch, Frontoparietal connectivity and hierarchical structure of the brain's functional network during Sleep, Frontiers in Neurology, vol. 3, no. 80, pp., 2012.

[19] F. J. P. Langheim, M. Murphy, B. A. Riedner, G. Tononi, Functional connectivity in slow-wave sleep: identification of synchronous cortical activity during wakefulness and sleep using time series analysis of electroencephalographic data, J Sleep Res., vol. 20, no. 4, pp. 496-505, 2011.